In this Supplement additional figures are shown supporting the discussion in the main paper.

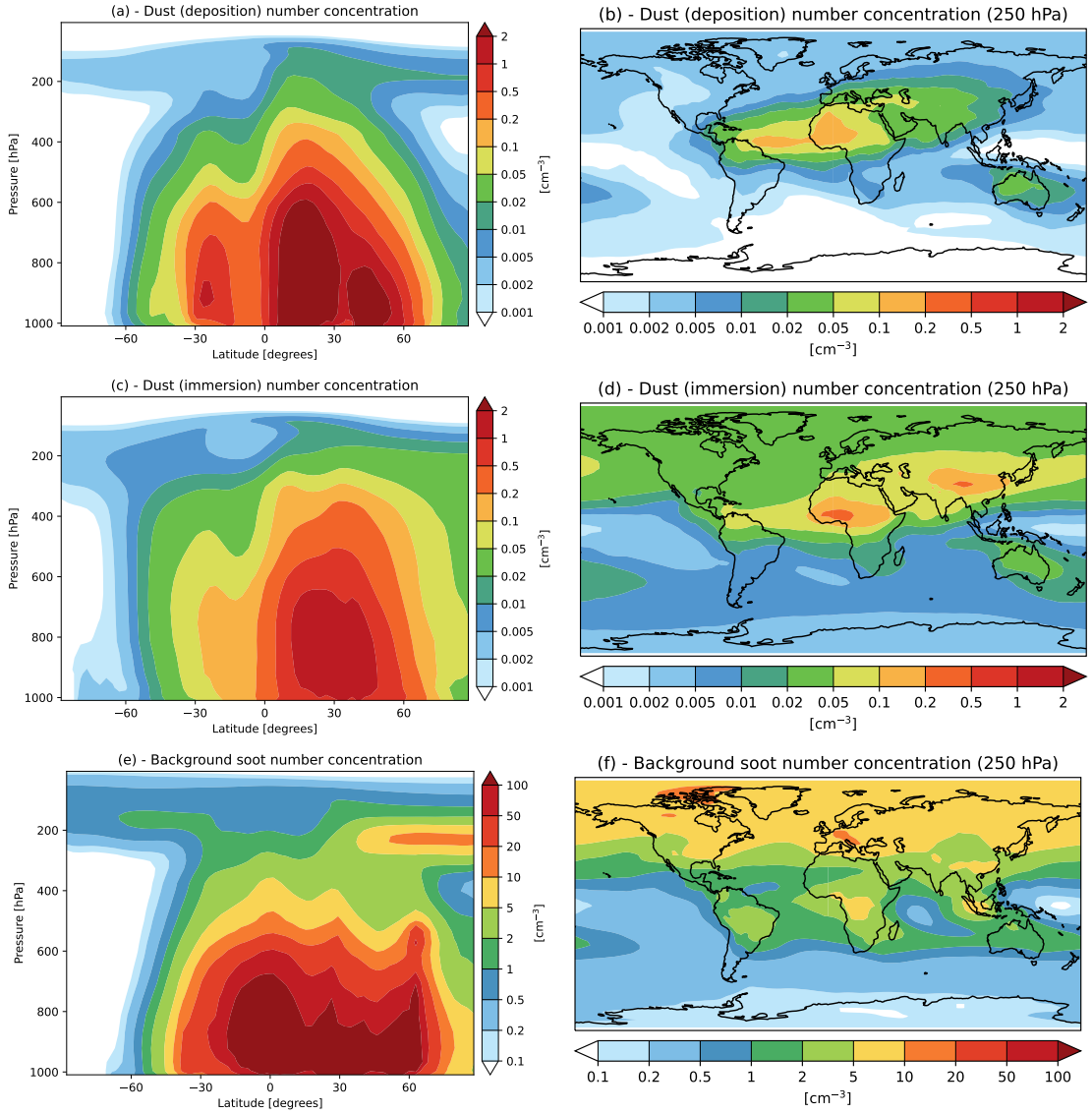

Figure S1: Multi-year average (2001–2015) number concentration of mineral dust in the deposition mode (a,b), mineral dust in the immersion mode (c,d), and background soot (i.e., from all sources except aviation, e,f). Panels (a), (c) and (e) show the zonal mean concentrations, while (b), (d), and (f) show the concentrations at about 250 hPa. The number concentration of INPs for each type is obtained after multiplying by the active fraction f_{act} of each type, as explained in the main paper.

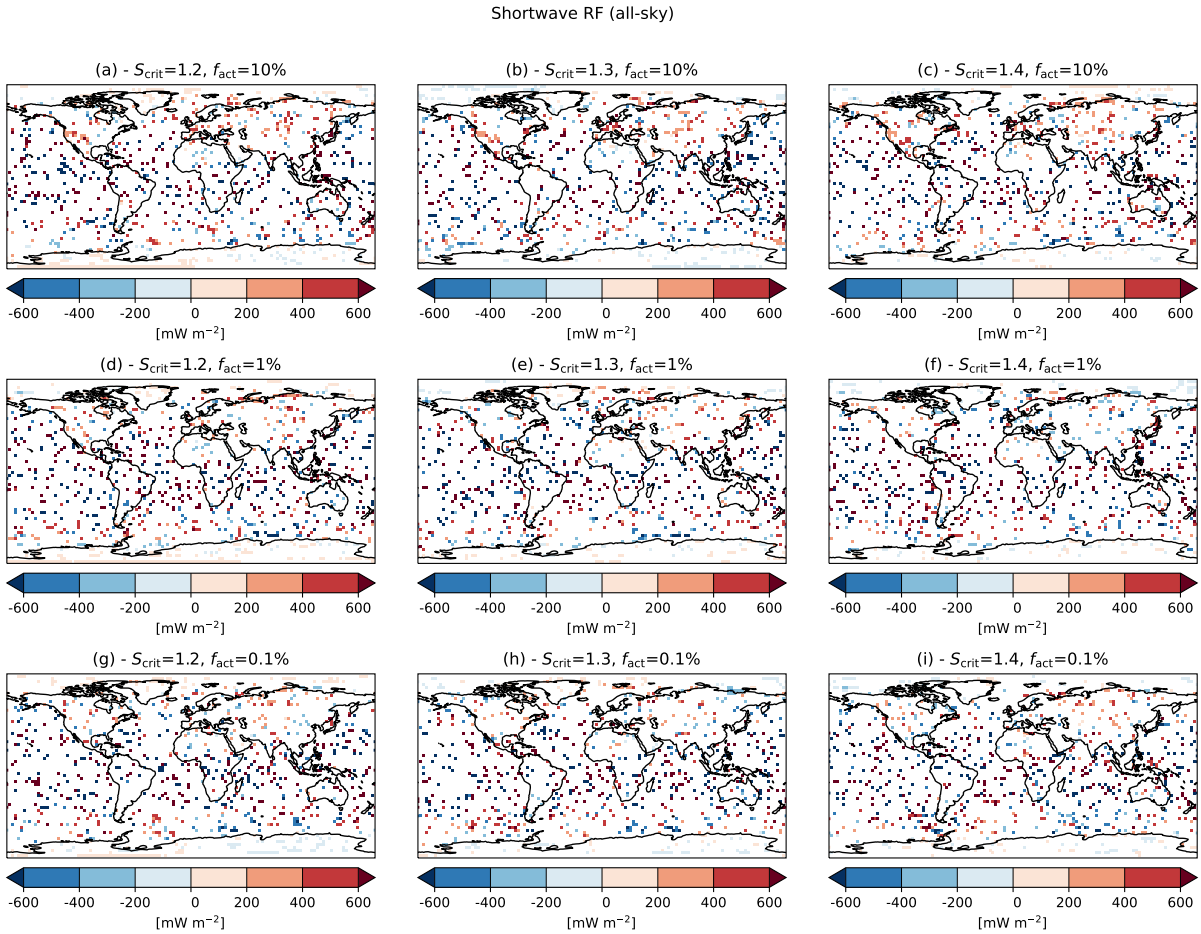

Figure S2: Multi-year average (2001–2015) top-of-the-atmosphere all-sky shortwave radiative forcing due to the effect of aviation soot on natural cirrus clouds, under different assumptions for the ice nucleation efficiency of aviation soot INPs (a-i). Grid-boxes with a statistical significance below 90% are masked out in white.

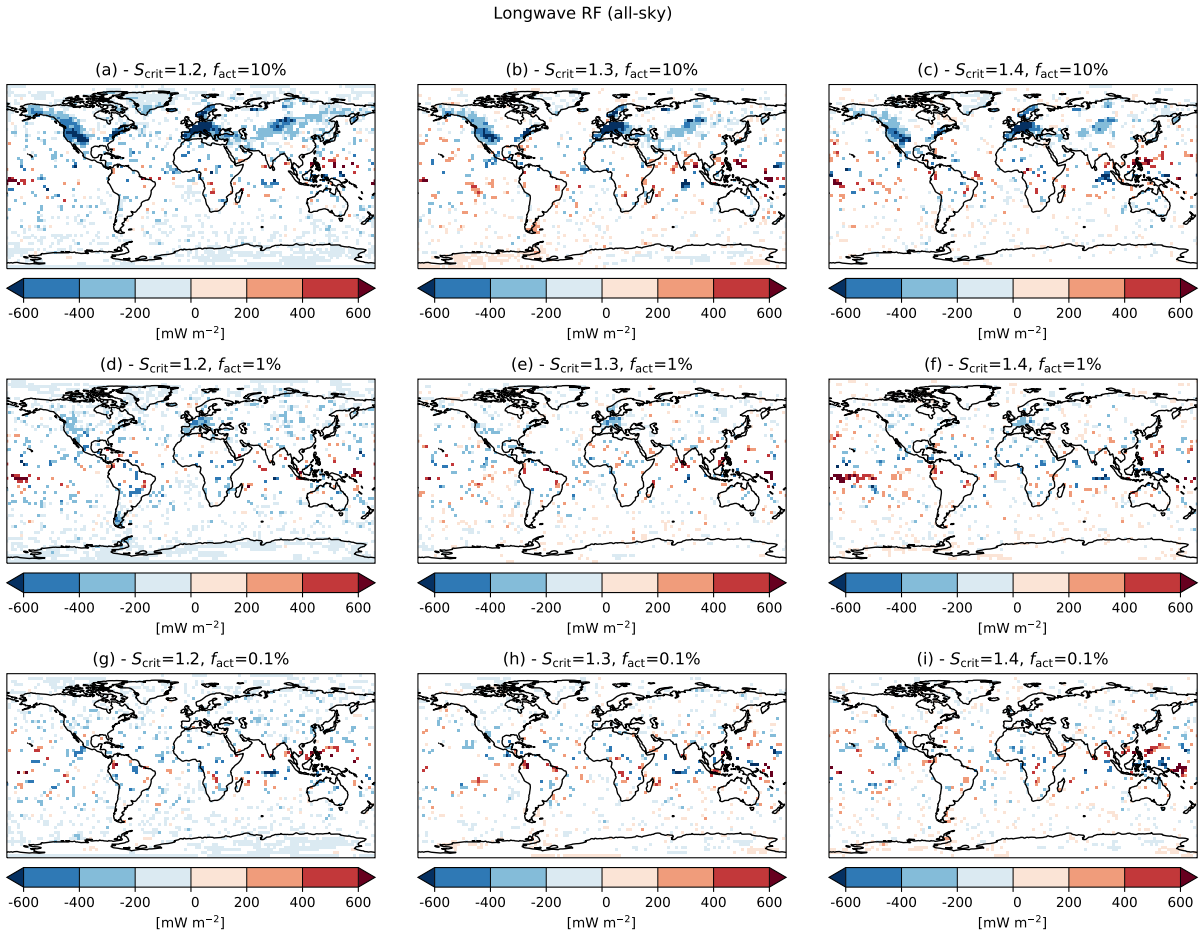

Figure S3: As in Fig. S2, but for all-sky longwave radiative forcing.

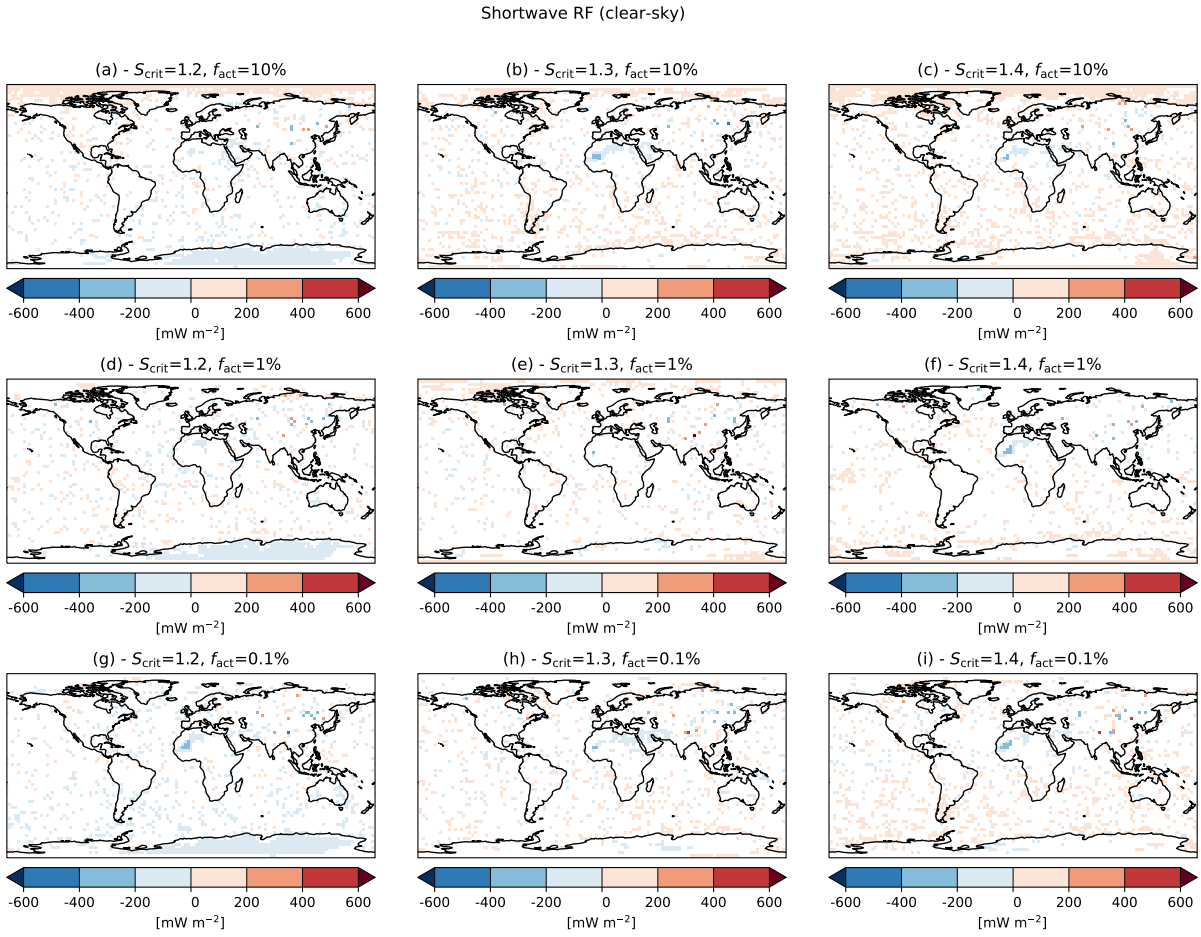

Figure S4: As in Fig. S2, but for clear-sky shortwave radiative forcing.

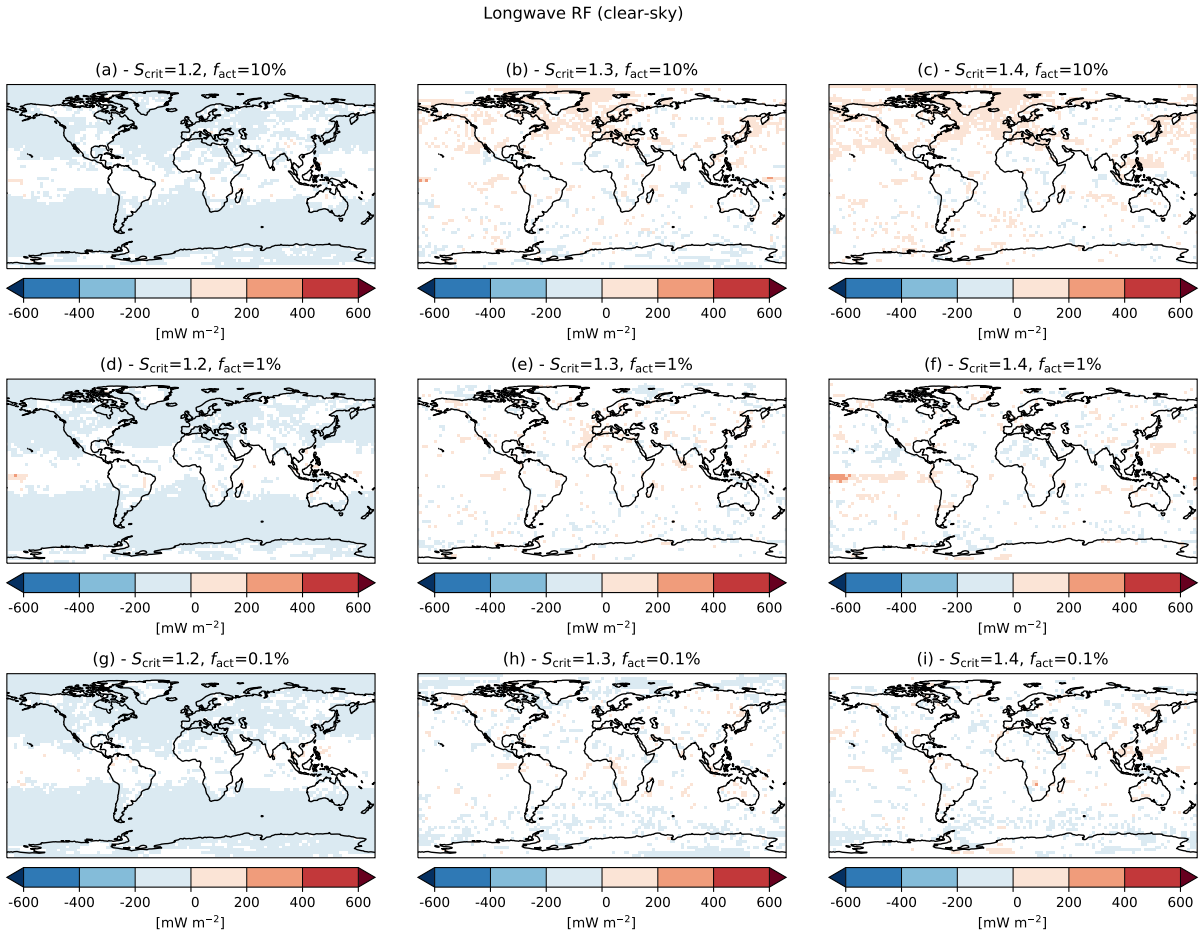

Figure S5: As in Fig. S2, but for clear-sky longwave radiative forcing.

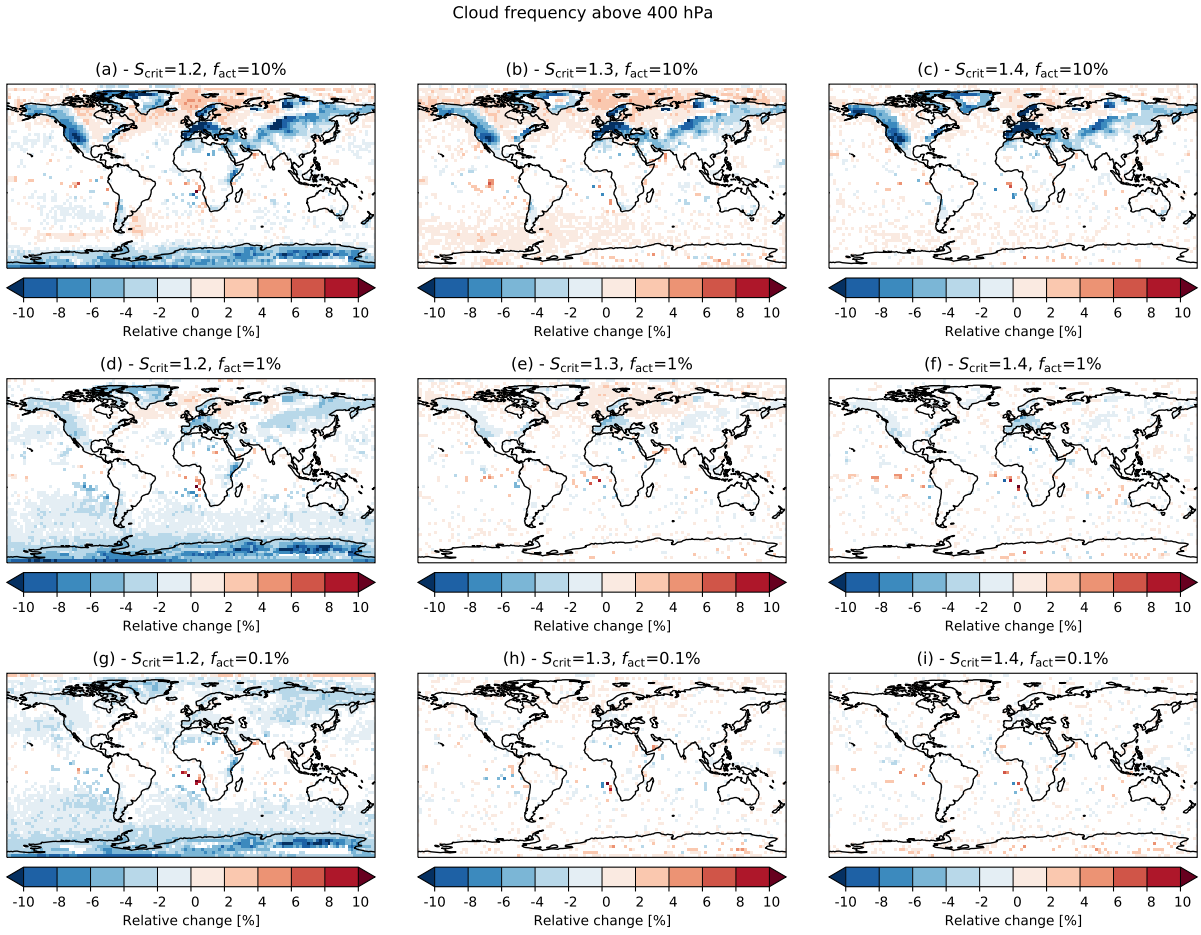

Figure S6: As in Fig. S2, but for cloud frequency above 400 hPa.

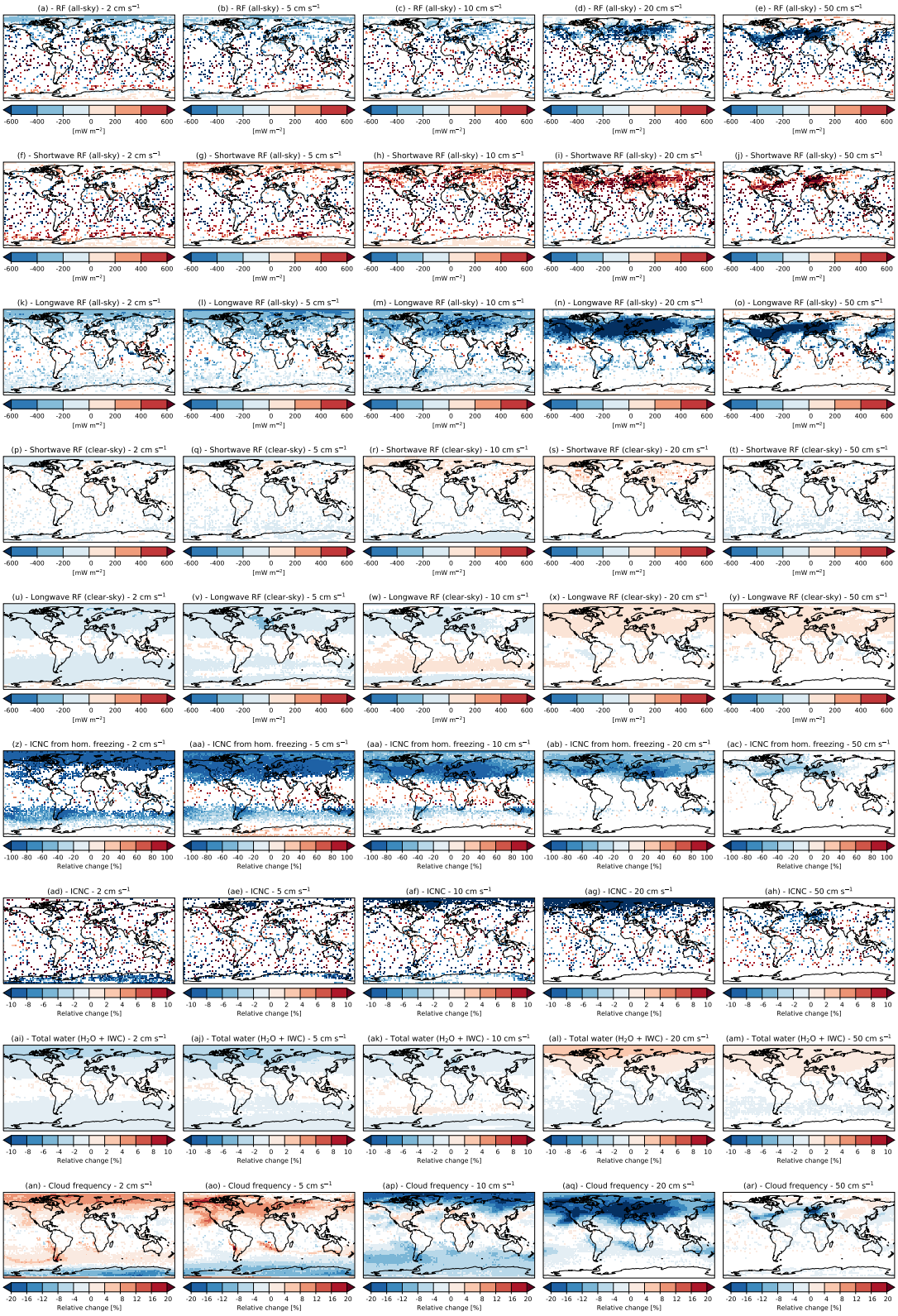

Figure S7: Multi-year average (2001–2015) top-of-the-atmosphere radiative forcings and changes in other relevant cloud properties due to the effect of aviation soot on natural cirrus clouds, under different values of prescribed vertical velocity. Grid-boxes with a statistical significance below 90% are masked out in white.